Tribology Letters (2021) 69:59
https://doi.org/10.1007/s11249-021-01432-y

ORIGINAL PAPER

Stress Relaxation of Comb Polymer Melts

Sidath Wijesinghe[1] · Dvora Perahia[1] · Ting Ge[2] · K. Michael Salerno[3] · Gary S. Grest[4]

Received: 5 February 2021 / Accepted: 30 March 2021 / Published online: 15 April 2021

Abstract
Branched polymers stress relaxation is at the center to their function as viscosity modifiers, though the fundamentals that underlie the correlation between the polymer topology and their impact on viscosity remains an open question. Here, the stress relaxation of short, branched polyethylene comb polymer melts is studied by molecular dynamics simulations. A coarse-grained model where four methylene groups constitute one bead is used, and the results are transposed to the atomistic level. For arms of length comparable to entanglement length n_e of the linear polymer, we show that while increasing the number of branches with the same arm length decreases the plateau modulus, the terminal diffusive time does not change significantly. Increasing the arm length decreases the plateau modulus and increases the terminal time. As arms shorter than n_e relax by the entanglement time, both the chain mobility and stress relaxation can be described by reptation of the backbone with an increased tube diameter and an increased friction coefficient; or in other words, the branches act as a solvent.

Graphic Abstract

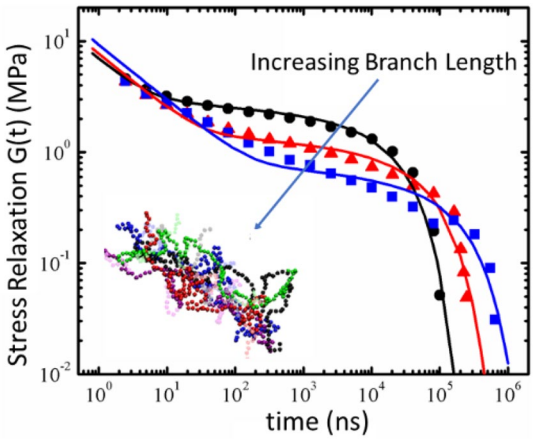

Keywords Comb Polymers · Stress relaxation · Molecular dynamics simulations

1 Introduction

The addition of a small number of side branches to flexible, linear polymer chains have dramatic effects on the viscosity and shear response of melts [1–3]. Varying the number and length of the branches tethered to the backbone of these comb polymers provides a pathway to control their rheological properties. The immense impact of polymers topology on processing of macromolecules has driven numerous experimental studies, all demonstrating significant effects of the branches on the flow characteristics of the melts [4–15]. These studies show that the dependence of the stress relaxation and shear viscosity on the number and length of the branches is rather convoluted. For example, the storage and loss moduli for combs with short branches measured

✉ Dvora Perahia
dperahi@g.clemson.edu

✉ Gary S. Grest
gsgrest@sandia.gov

Extended author information available on the last page of the article

at different temperatures could be superimposed onto a universal curve with a simple shift, however, long-chain branching results in thermo-rheological complexity in which the data cannot be superimposed by a simple temperature shift [7, 9, 10].

On time scales longer than that for the branches to relax, the motion of well entangled comb polymers follow the reptation model [16, 17], in which the polymer chain confined in a tube of neighboring chains, moves cooperatively along the tube axis, commonly referred to as the primitive path. After the branches relax, the branches act as an effective solvent for the backbone while concurrently providing a drag on the motion of the backbone [1, 2, 18]. For comb polymers with short branches, comparable to the entanglement molecular weight of the linear backbone, the dominant contribution to the chain mobility and stress relaxation is from the entangled backbone. In this case, comb polymers behave as reptating chains with increased tube diameter d_T. For longer arms, the stress relaxation is more complex as the branch segments near the branch point relax on a time scale which depends exponentially on the arm length. This gives rise to an effective tube diameter which grows as the side branches relax. Only after the arms fully relax, does the backbone relax [6, 11, 18] and the backbone entanglements ultimately control the chain mobility and stress relaxation.

While there have been numerous experimental studies of stress relaxation of comb polymers, the local dynamics that governs the macroscopic motion of the polymers has not been realized. Limited number of numerical simulations have recently probed the local motion of comb polymers. Bačová et al. [19, 20] showed that in asymmetric stars and combs with two branches, the branch point movements can be described as the motion over a network of traps. Zhou and Larson [21] simulated asymmetric star polymers using a coarse grained model and showed that for time scales less than the short-arm relaxation time, the branch point remains anchored within a length scale of a tube diameter. Once the short arm relaxes, the branch point takes a random hop along the confining tube. Wijesinghe et al. [22] carried out molecular dynamics simulations for a coarse grained model for entangled polyethylene comb polymers. They showed that as the branch length increases, the combination of arm retraction and backbone mobility leads to a wide spectrum of arm relaxation times and that the motion of the polymer backbone is well described by repetition over intermediate time scales. They also showed that the tube diameter and the entanglement time, directly measured from the crossover from the early time Rouse to reptation regime, both increase linearly with the length of the branches. However, none of these numerical studies have been able to resolve the stress relaxation of comb polymers, critical to the understanding of the mechanism in which topology of polymers affect their stress release.

Here, we probe the effects of branching on the dynamics of melts of loosely branched comb polymers with branches of length comparable to the entanglement molecular weight M_e using molecular dynamics (MD) simulations. The branches are sparsely distributed along the backbone, so that they do not affect the end-to-end distance of the polymer. We study the stress relaxation of melts of entangled comb polymers with multiple short branches. MD simulations allow us to visualize and study the microscopic behavior that underlies macroscopic experimental observations. Given the broad time and length scales associated with the polymeric motion, we adopt a coarse grained (CG) model for polyethylene, where 4 methylene groups are represented by one bead, to capture the mobility and stress relaxation of loosely branched polyethylene melts on multiple time and length scales. This model captures well the diffusion, plateau modulus and viscosity of entangled, linear polyethylene melts [23, 24]. The results presented here add an important facet to our previous results on the mobility of comb polymers. The molecular motion of these branched polymers is captured through reptation model with a tube diameter that increases as the length of the branches increases, illustrated by the chain snapshots shown in Fig. 1.

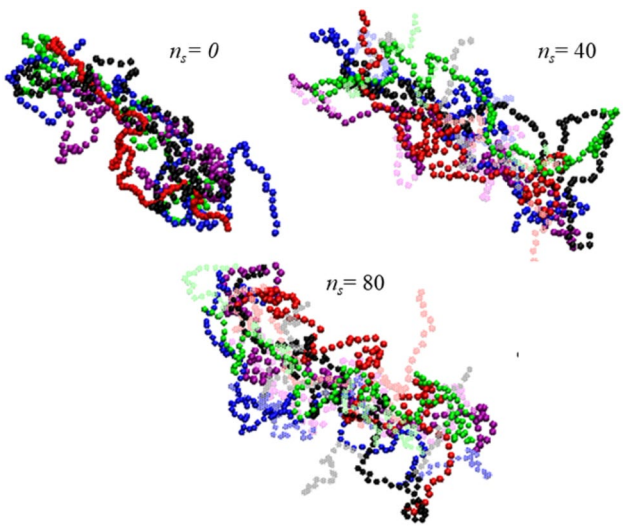

Fig. 1 Visualization of a coarse grained model of a polyethylene chain with backbone of n = 480 carbons (120 CG beads) plotted five times (different colors), each separated by 62 ns. The chains have n_b = 4 randomly placed branches of length n_s = 0, 40, and 80 carbon atoms (0, 10, 20 and 40 CG beads). Backbone is plotted in dark color while side chains are translucent

2 Model and Methodology

A CG model for polyethylene with four methylene groups per CG bead (coarse graining degree $\lambda_c = 4$) previously derived by Salerno et al. was used for the current study [23, 25, 26]. The interaction potential between CG beads was derived from an atomistic simulation for a linear chain melt of $C_{96}H_{194}$ at density $\rho = 0.76$ g/cm^3 and temperature $T = 500$ K using an iterative Boltzmann procedure. The atomistic simulations used the optimized potentials for liquid simulations (OPLS) force fields of Jorgensen et al. [27, 28] with modified dihedral coefficients to better reproduce the properties of long alkanes [29]. In the CG model nonbonded interactions are truncated at 1.0 nm. All simulations were run at constant volume using a velocity-Verlet integrator with a time step of 20 fs. A Langevin thermostat [30, 31] with damping time constant of 20 ps maintains the temperature at 500 K. Periodic boundary conditions were used in all three directions. All simulations use the large atomic molecular massive parallel simulator (LAMMPS) molecular dynamics code [32]. Detailed descriptions of the CG development is given by Salerno et al. [23, 25] and Peters et al. [26].

As coarse graining reduces the number of degrees of freedom, the free-energy landscape is much smoother compared to fully atomistic simulations. This results in an increase in the mobility of the chains in the CG models compared to the fully atomistic model [25]. For $\lambda_c = 4$ at 500 K, Salerno et al. [25] showed that the mean squared displacement in the atomistic and CG model for melts of linear chains with $n = 96$ and 480 carbons overlapped if time in the CG model is scaled by a dynamic scaling factor $\alpha = 6.2$. We use this value of α to scale time for the comb polymers.

The PE comb polymer melts were prepared as described in Wijesinghe et al. [22]. Our previous study was able to resolve mobility and viscosity for melts of chains with $n = 480$ backbone carbons (120 CG beads) and $n = 1920$ backbone carbons (480 CG beads) with $n_b = 4$ to 16 randomly placed branches of length $n_s = 0$–160 carbons (0–40 CG beads). Here we probe the stress relaxation of the longer chain melts with 800 chains of length $n = 1920$ backbone carbons with $n_b = 16$ randomly placed branches of length $n_s = 0$, 40, and 80 and $n_b = 16$, 32 and 64 branches of length $n_s = 40$. For all values of n_s and n_b studied here, these chains are in the comb regime where the branches do not affect the polymer backbone rigidity, as reflected in a nearly constant mean squared radius of gyration $< R_g^2 >$ [22]. For linear polyethylene chains, this CG models reproduces quite well the single chain statistics including the mean squared end-to-end distance $< R^2 > / M_w = 1.29 \pm 0.02$ Å^2/(g/mol) which is in good agreement with the experimental value of 1.21 Å^2/(g/mol) obtained from small-angle neutron scattering at 443 K and packing length $p = (\rho_{chain} < R^2 >) = 1.8$ Å compared to the experimental value of $p = 1.69$ Å at 413 K [33]. For reference, the experimentally [34, 35] measured entanglement molecular weight M_e of linear polyethylene without branches is 1.1 − 1.2 kg/mol or about $n_e = 80$ (20 CG beads). Hence, the comb polymers studied here are well entangled with $Z = n/n_e = 24$ while the length of the side branches are relatively short, $n_s = 0$, $n_e/2$ and n_e. Here n_e is the entanglement strand length for linear polymers, the effective n_e for the backbone of the comb polymers is larger as suggested by the lower plateau modulus.

The stress relaxation modulus was measured for each system using the Green–Kubo relation where $\sigma_{\alpha\beta}(t)$ are the off-diagonal components xy, xz and yz of the stress, V is the volume of the system and t is time. Results for $G(t)$ presented here are an average of the three components. We also measured the normal stress decay after deforming polymer chains in a melt by a small step strain [36, 37]. This was done by applying a uniaxial elongation to deform the simulation cell in the x-direction $L_x = \lambda L$ while shrinking the simulation cell in the other two directions $L_y = L_Z = L/\sqrt{\lambda}$ to keep the density of the system constant. Using the stress–strain description for classical rubber elasticity [38], the stress relaxation modulus is given by

$$G(t) = \frac{\sigma_{xx}(t) - \frac{1}{2}\left(\sigma_{yy}(t) + \sigma_{zz}(t)\right)}{\lambda^2 - 1/\lambda} \quad (1)$$

Here, we use $\lambda = 1.1$ and 1.2 following Hsu and Kremer [36] who applied this method to determine $G(t)$ for the standard bead spring model [39].

3 Results

To distinguish the relevant time scales and different scaling regimes, we first consider the effect adding multiple branches on the chain mobility. Previously we considered the effect of increasing the branch length n_s, here we present new results for increasing number of branches n_b. The mean squared displacement (MSD) of chains in equilibrated melts was calculated for the center six beads, $g_1(t) = < (r_i(t) - r_i(0))^2 >$ to suppress the fluctuations caused by chain ends and for the center of mass (cm) of the chains, $g_3(t) = < (r_{cm}(t) - r_{cm}(0))^2 >$, where $r_i(t)$ is the position of atom i at time t, and $r_{cm}(t)$ is the position of the center of mass of the chains. Figure 2 shows results for the MSD of chains of $n = 1920$ carbon atoms (480 CG beads) with a different number of branches n_b each with branch length $n_s = 40$. These data show that the number of branches has only a small effect on chain mobility in the comb regime. They also show the

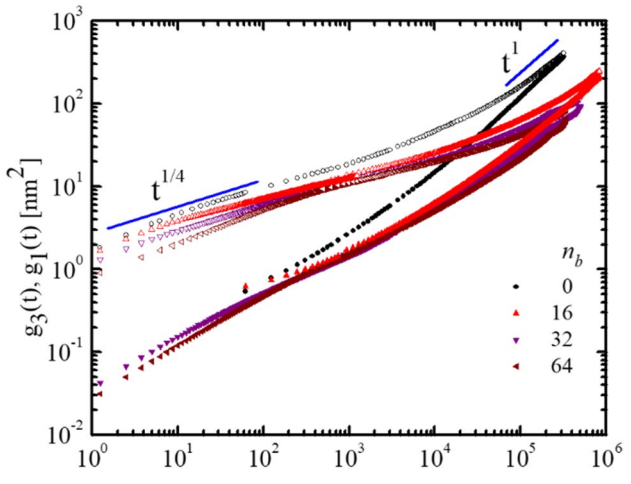

Fig. 2 Mean-squared displacement (MSD) of the center six CG beads $g_1(t)$ (open symbols) and of the center of mass $g_3(t)$ (full symbols) for chains of $n=1920$ carbon atoms for the indicated number of branches n_b of lengths $n_s=40$. The solid lines represent the scaling predictions t^1 for the diffusive regime and $t^{1/4}$ for the reptation regime

distinctive $t^{1/4}$ scaling regime in $g_1(t)$ at intermediate times, which arises from the relaxation dynamics of the backbone confined in the tube. At later times the MSD increases as t^1 in the diffusive regime. The diffusive time τ_d, determined from the time that the inner beads have moved a distance comparable to the size of the chain $g_1(\tau_d)=3<R_{gb}{}^2>$, increases only slightly with increasing n_b. Here, $<R_{gb}{}^2>$ is the mean squared radius of gyration of the backbone.

The effect of increasing the length of the branches is much stronger than that of increasing the number of branches. We previously showed [22] that the extent of the $t^{1/4}$ scaling regime increases with increasing branch length n_s. The tube diameter d_T and entanglement time τ_e, extracted from the crossover from the early time $t^{1/2}$ Rouse regime to the $t^{1/4}$ scaling regime in $g_1(t)$ both increase linearly with increasing branch length n_s, while the diffusive time τ_d, increased exponentially with increasing branch length [22]. Figure 1 illustrates this increase in d_T with increasing chain length of the branches n_s. For illustration we show results for $n=480$, though all the results in this paper are longer chains with $n=1920$ backbone carbons.

In the reptation mode, the polymer chain confined in a tube moves coherently along the primitive path, after all internal dynamic modes have been relaxed. The primitive path length scales with the entanglement length as $L_{pp} \sim {}^1/_{n_e^{1/2}}$. The friction coefficient ζ of the chain scales linearly with the number of monomers in the chain. The reptation time τ_d is the time for the chain to diffuse a distance L_{pp}, and scales as $\tau_d \sim L_{pp}^2\zeta \sim \zeta/n_e$. In the approximation of a comb polymer with short branches as an effective linear polymer, both ζ and n_e are increased by the addition of side branches. Since short branches undergo Rouse dynamics, the overall chain friction coefficient ζ is nevertheless proportional to the number of monomers, which is increased by the additional monomers of the branches.

The relaxation time of the branches compared to the backbone has a strong effect on both the chain mobility and stress relaxation. We measured the autocorrelation function of the end-to-end vector of the branches and extracted the branch relaxation times τ_a [22]. For $n_s=40$, the time for the arms to relax $\tau_a \sim 13$ ns, is much shorter than the time $\tau_e \sim 50$ ns to reach the reptation regime, while for $n_s=80$, $\tau_a \sim 100$ ns, which is comparable to τ_e [22] for $n_s=80$. That the arm relaxation times are comparable to or shorter than τ_e supports our finding that these comb polymers with short arms behave as reptating chains with increased tube diameter.

The stress response function after a small perturbation $G(t)$ is an important experimental measure of polymer rheology. For long entangled linear polymers, at short times $G(t)$ decays as the chains locally relax in response to the perturbation like any fluid. However, for intermediate times $G(t)$ plateaus at $G_N^o = \frac{4}{5}\rho RT/M_e$ This plateau region in $G(t)$ occurs for intermediate times where the chains are assumed to move in a tube due to entanglements from the other chains. Only after the chains have reached the diffusive regime, does $G(t)$ relax to zero at a time τ_d. For short branches, the relaxation time is shorter than the time τ_d for the backbone to feel the effect of entanglements from other chains. In this case, the branches only affect the very early decay of $G(t)$. Short branches increase the effective tube diameter d_T and entanglement time τ_d, and thus allow more internal dynamics modes to relax without being affected by the tube. The dominant contribution to the stress relaxation in this case of short branches is from the entangled backbone. For branches longer than n_e, the stress relaxation is more complex as the branch segments near the branch point relax on time scale which depends exponentially on the branch length. This gives rise to an effective tube diameter which grows as the side branches relax. Only after the branches fully relax, does the backbone relax [6, 11, 18].

The relaxation modulus was measured from equilibrium stress autocorrelations and from stress relaxation after small strain. Figure 3a shows $G(t)$ measured from the stress autocorrelation function for comb polymers $n_b=16$, 32 and 64 branches of length $n_s=40$ and Fig. 3b shows G(t) for branch lengths $n_s=0$, 40, and 80 with $n_b=16$ branches. As the number of branches n_b increases the plateau modulus G_N^o decreases while terminal time τ_d is approximately unchanged. Increasing the length of the side branches n_s leads to a decrease in G_N^o and an increase in τ_d. To quantify the changes in the plateau modulus, $G(t)$ for the short branched comb polymers studied here was fit to a modified Likhtman-McLeish (LM) expression [40], which combines self-consistent theories for contour length fluctuations and constraint release with reptation theory,

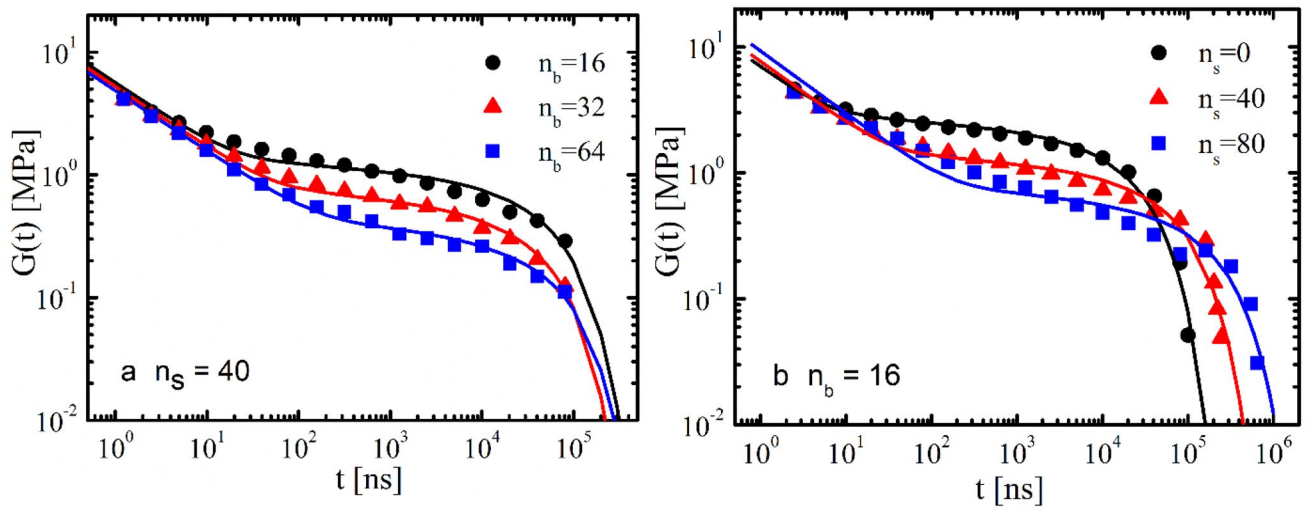

Fig. 3 Stress relaxation function $G(t)$ for comb polymers with backbone of n = 1920 carbons for melts with a) $n_b = 16$, 32 and 64 branches of length $n_s = 40$ and b) branch lengths $n_s = 0$, 40, and 80 with $n_b = 16$ branches. Solid lines are fit to eqs. 2 and 3

$$G(t) = \frac{k_B T}{n\nu}\left[\frac{1}{5}\sum_{p=1}^{Z}\left(4\mu(t)R(t) + e^{-tp^2/\tau_R}\right) + \sum_{p=Z+1}^{N} e^{-2tp^2/\tau_R}\right] \quad (2)$$

Here, $\mu(t)$ and $R(t)$ account for single- and multi-chain relaxation processes of the tube model and n is the total number of CH_2 monomers in the system. The key quantity in this expression is the single-chain memory function $\mu(t)$ for the fraction of the primitive chain which has not escaped from its original tube after a time t. For $\mu(t)$, we use the Doi-Edwards reptation stress relaxation function [17]

$$\mu(t) = \frac{8}{\pi^2}\sum_{q=1,odd}^{\infty}\frac{1}{q^2}\exp\left(-\frac{q^2 t}{\tau_d}\right) \quad (3)$$

For $R(t)$, we use the double-reptation expression for constraint release $R(t) = \mu(t)$ [41, 42]. The three fitting parameters are the number of entanglements per chain Z, the terminal relaxation time τ_d, and the Rouse time τ_R. As Z is related to the mode index and has to be an integer. In the fitting, Z is varied over integer values to obtain the best fit. The volume of a CH_2 monomer is $\nu = 0.031$ nm^3 for $\rho = 0.76$ g/cm^3. Equations 2 and 3are appropriate for the systems studied here since the arms relax on a time scale shorter than that for the backbone of feel mutual entanglements from other chains. For branches longer than n_e, one has to include the fact that the tube diameter d_T increases and the effective entanglement length n_e increases as the branches relax so that the total primitive path length becomes dependent on the current extent of relaxation of the branches [6, 11, 18].

As the number of branches increase from 16 to 64, the plateau modulus G_N^o decreases approximately linearly, G_N^o= 1.13 MPa, 0.66 MPa and 0.38 MPa for $n_b = 16$, 32 and 64, respectively. For comparison, $G_N^o = 2.45$MPa for linear polymers. The entanglement time τ_e increases with increasing n_b, $\tau_e = 40$ ns, 101 ns and 265 ns for $n_b = 16$, 32 and 64, respectively. From the fit to eqs. 2 and 3, the longest relaxation times $\tau_d \sim 1.5\times10^5$ ns are independent of the number of branches within the error of our measurements. The diffusive time $\tau_d \sim 5\times10^5$ ns extracted from the MSD of the center backbone beads (Fig. 2) agrees very well with that found from the stress relaxation. These results show that as the number of branches increases, the ratio ζ/n_e and thus τ_d remains almost unchanged.

As the length of the branches increases, the plateau modulus G_N^o also decreases linearly with increasing n_s, G_N^o= 2.45 MPa, 1.22 MPa and 0.66 MPa for branch length $n_s = 0$, 40 and 80, respectively. As seen in Fig. 4, the relaxation times describing the stress relaxation are in excellent agreement with those extracted from the MSD, supporting the idea that for these short comb polymers can be treated as linear chains with a larger tube diameter. The Rouse time does not change much with increasing branch length, as it is the relaxation time of the internal dynamic modes along the backbone, which are not affected by the branches.

Fetters et al. [33, 34] have shown that for a wide range of flexible linear Gaussian chains, the entanglement molecular weight M_e can be expressed as a universal power law of the packing length p,

$$M_e = n_t^2 N_A \rho p^3 \quad (4)$$

where N_A is the Avogadro number. Fetters et al. [34] found that the coefficient n_t is insensitive to temperature and equal to 19.1 ± 1.4 (assuming $M_e = \frac{4}{5}\rho RT/G_N^o$). As seen in Fig. 5, the backbone entanglement length M_e scales with p^3 as

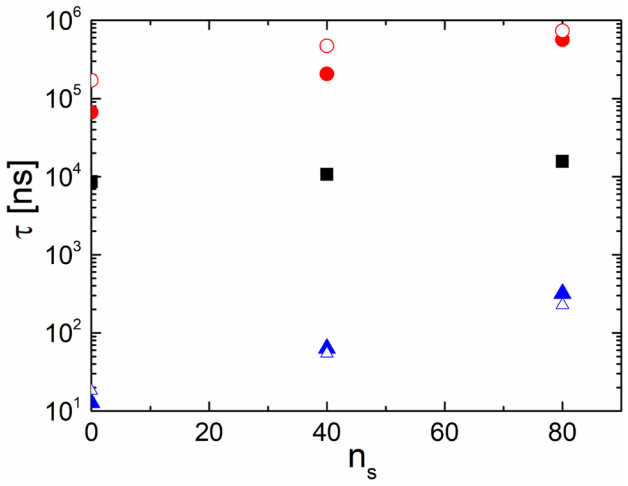

Fig. 4 Entanglement time τ_e (blue triangles) Rouse time, τ_R (black square) and diffusive time τ_d (red circles) as a function of length of the branches extracted from the MSD (open) and from $G(t)$ (filled). Length of the backbone $n=1920$ carbons with $n_b=16$ branches. Error bars are size of symbols

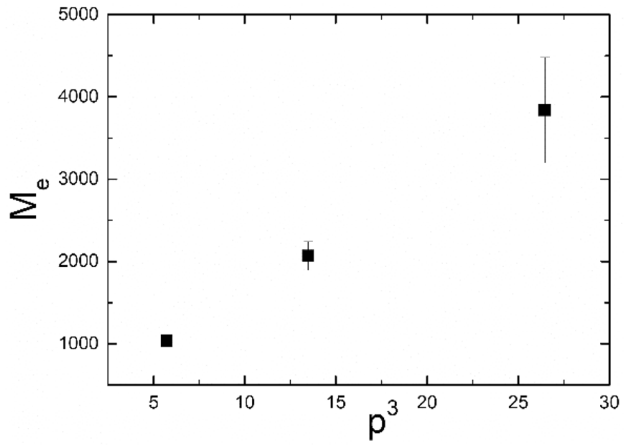

Fig. 5 Entanglement molecular weight M_e of the backbone as a function of the packing length p

predicted for flexible linear chains. The best fit to the coefficient $n_t=16.4\pm0.1$. Combs with $n_b=32$, $n_s=16$ and $n_b=16$, $n_s=40$ have the same packing length p and the same plateau modulus from the best fits to $G(t)$ as predicted by Eq. 4. This further supports the idea that the combs with short chains behave as reptating chains with increased tube diameter.

Determination of the stress relaxation function $G(t)$ from fluctuations in the off-diagonal components of the stress tensor requires long simulations, usually several times longer than the longest relaxation time, to obtain reliable results. An alternative method is to follow the experimental procedure and apply a small strain and measure stress relaxation. Although computationally more efficient, the challenge is to apply a strain large enough to reliably measure the stress yet remain in the linear response regime [36, 37]. As seen in Fig. 6, the results for the two methods agree nicely for the two methods when the step strain is small ($\lambda=1.1$). For larger strain, as shown in the inset of Fig. 5, application of a strain of 20% overestimates $G(t)$ for $n_b=16$ and 32, though not for $n_b=64$.

4 Conclusions

The effect of the number of branches and branch length on the chain mobility and stress relaxation of short-branched polyethylene comb polymer melts with short branches has been studied. We find that the presence of sparsely placed branches greatly reduces the chain mobility of comb polymers compared to their linear analogs. The short branches act as an effective solvent for the backbone and increase the tube diameter and the entanglement time. While increasing the number of branches has only a small effect on the chain mobility and the terminal relaxation time, the plateau modulus decreases linearly with the number of branches. Increasing the branch length significantly reduces the chain mobility and plateau modulus. The entanglement time τ_e and terminal relaxation times t_d extracted from the chain mobility and from the stress relaxation are in very good agreement.

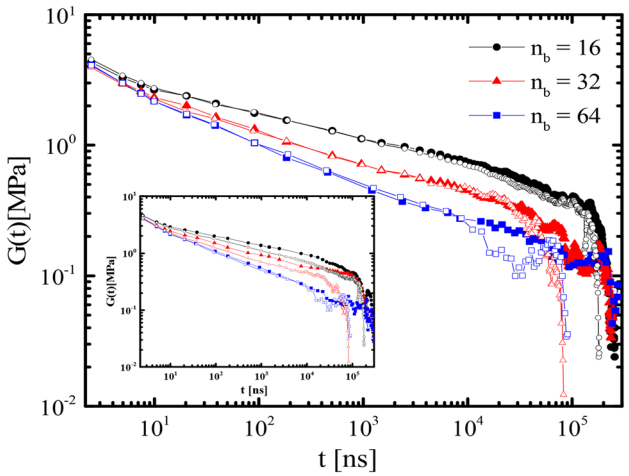

Fig. 6 Comparison of stress relaxation function $G(t)$ measured from the Green–Kubo relationship (filled symbols) and from step strain with $\lambda=1.1$ (Eq. 1) (open symbols) for comb polymers with $n_b=16$, 32 and 64 branches of length $n_s=40$. Inset compares results for $\lambda=1.1$ (open symbols) and 1.2 (filled symbols)

Acknowledgement We dedicate this paper to the memory of Mark O. Robbins, graduate advisor to two of us (TG and KMS), friend and colleague to all. D. Perahia kindly acknowledged NSF DMR 1905407 for partial support. T. Ge acknowledges start-up funds from the University of South Carolina. This research used resources of the National Energy Research Scientific Computing Center (NERSC), a U.S. Department of Energy Office of Science User Facility operated under Contract No. DE-AC02-05CH11231. This work was performed, in part, at the Center for Integrated Nanotechnologies, an Office of Science User Facility operated for the U.S. Department of Energy (DOE) Office of Science. Sandia National Laboratories is a multimission laboratory managed and operated by the National Technology and Engineering Solutions of Sandia, LC, a wholly owned subsidiary of Honeywell International, Inc., for the U.S. Department of Energy's National Nuclear Security Administration under contract no. DE-NA-0003525. The views expressed in the article do not necessarily represent the views of the U.S. DOE or the United States Government.

References

1. McLeish, T.C., Milner, S.T.: Entangled dynamics and melt flow of branched polymers. In: Roovers, J. (ed.) Branched Polymers II Advances in Polymer Science, pp. 195–256. Springer, Berlin (1999)
2. Snijkers, F., Pasquino, R., Olmsted, P., Vlassopoulos, D.: Perspectives on the viscoelasticity and flow behavior of entangled linear and branched polymers. J. Phys. Condens. Matter **27**, 473002 (2015)
3. Matyjaszewski, K.: Architecturally complex polymers with controlled heterogeneity. Science **333**, 1104–1105 (2011)
4. Fujimoto, T., Narukawa, H., Nagasawa, M.: Viscoelastic properties of comb-shaped polystyrenes. Macromolecules **3**, 57–64 (1970)
5. Roovers, J., Graessley, W.: Melt rheology of some model comb polystyrenes. Macromolecules **14**, 766–773 (1981)
6. Daniels, D., McLeish, T., Crosby, B., Young, R., Fernyhough, C.: Molecular rheology of comb polymer melts. 1. Linear viscoelastic response. Macromolecules **34**, 7025–7033 (2001)
7. Lohse, D., Milner, S., Fetters, L., Xenidou, M., Hadjichristidis, N., Mendelson, R., Garcia-Franco, C., Lyon, M.: Well-defined, model long chain branched polyethylene. 2. Melt rheological behavior. Macromolecules **35**, 3066–3075 (2002)
8. Kapnistos, M., Vlassopoulos, D., Roovers, J., Leal, L.: Linear rheology of architecturally complex macromolecules: comb polymers with linear backbones. Macromolecules **38**, 7852–7862 (2005)
9. Stange, J., Uhl, C., Münstedt, H.: Rheological behavior of blends from a linear and a long-chain branched polypropylene. J. Rheo. **49**, 1059–1079 (2005)
10. Stadler, F.J., Gabriel, C., Münstedt, H.: Influence of short-chain branching of polyethylenes on the temperature dependence of rheological properties in shear. Macromol. Chem. Phys. **208**, 2449–2454 (2007)
11. Inkson, N., Graham, R., McLeish, T., Groves, D., Fernyhough, C.: Viscoelasticity of monodisperse comb polymer melts. Macromolecules **39**, 4217–4227 (2006)
12. Wagner, M.H., Rolón-Garrido, V.H., Hyun, K., Wilhelm, M.: Analysis of medium amplitude oscillatory shear data of entangled linear and model comb polymers. J. Rheol. **55**, 495–516 (2011)
13. Kempf, M., Ahirwal, D., Cziep, M., Wilhelm, M.: Synthesis and linear and nonlinear melt rheology of well-defined comb architectures of PS and PpMS with a low and controlled degree of long-chain branching. Macromolecules **46**, 4978–4994 (2013)
14. Abbasi, M., Faust, L., Riazi, K., Wilhelm, M.: Linear and extensional rheology of model branched polystyrenes: from loosely grafted combs to bottlebrushes. Macromolecules **50**, 5964–5977 (2017)
15. Haugan, I.N., Maher, M.J., Chang, A.B., Lin, T.-P., Grubbs, R.H., Hillmyer, M.A., Bates, F.S.: Consequences of grafting density on the linear viscoelastic behavior of graft polymers. ACS Macro Lett. **7**, 525–530 (2018)
16. de Gennes, P.-G.: Reptation of a polymer chain in the presence of fixed obstacles. J. Chem. Phys. **55**, 572–579 (1971)
17. Doi, M., Edwards, S.F.: The Theory of Polymer Dynamics. Oxford University, Oxford (1986)
18. Yurasova, T., McLeish, T., Semenov, A.: Stress relaxation in entangled comb polymer melts. Macromolecules **27**, 7205–7211 (1994)
19. Bacová, P., Lentzakis, H., Read, D.J., Moreno, A.J., Vlassopoulos, D., Das, C.: Branch-point motion in architecturally complex polymers: estimation of hopping parameters from computer simulations and experiments. Macromolecules **47**, 3362–3377 (2014)
20. Bačová, P., Moreno, A.J.: Real-space analysis of branch point motion in architecturally complex polymers. Macromolecules **47**, 6955–6963 (2014)
21. Zhou, Q., Larson, R.G.: Direct molecular dynamics simulation of branch point motion in asymmetric star polymer melts. Macromolecules **40**, 3443–3449 (2007)
22. Wijesinghe, S., Perahia, D., Grest, G.S.: Polymer topology effects on dynamics of comb polymer melts. Macromolecules **51**, 7621–7628 (2018)
23. Salerno, K.M., Agrawal, A., Peters, B.L., Perahia, D., Grest, G.S.: Dynamics in entangled polyethylene melts. Eur. Phys. J. Special Top. **225**, 1707–1722 (2016)
24. Grest, G.S., Michael Salerno, K., Peters, B.L., Ge, T., Perahia, D.: Resolving properties of entangled polymers melts through atomistic derived coarse-grained models. In: Andreoni, W., Yip, S. (eds.) Handbook of Materials Modeling: Methods: Theory and Modeling, pp. 1397–1410. Springer, Cham (2020)
25. Salerno, K.M., Agrawal, A., Perahia, D., Grest, G.S.: Resolving dynamic properties of polymers through coarse-grained computational studies. Phys. Rev. Lett. **116**, 058302 (2016)
26. Peters, B.L., Salerno, K.M., Agrawal, A., Perahia, D., Grest, G.S.: Coarse grained modeling of polyethylene melts: effect on dynamics. J. Chem. Theory Comput. **13**, 2890–2896 (2017)
27. Jorgensen, W.L., Madura, J.D., Swenson, C.J.: Optimized intermolecular potential functions for liquid hydrocarbons. J. Am. Chem. Soc. **106**, 6638–6646 (1984)
28. Jorgensen, W.L., Maxwell, D.S., TiradoRives, J.: Development and testing of the OPLS all-atom force field on conformational energetics and properties of organic liquids. J. Am. Chem. Soc. **118**, 11225–11236 (1996)
29. Siu, S.W., Pluhackova, K., Böckmann, R.A.: Optimization of the OPLS-AA force field for long hydrocarbons. J. Chem. Theory Comput. **8**, 1459–1470 (2012)
30. Schneider, T., Stoll, E.: Molecular-dynamics study of a three-dimensional one-component model for distortive phase transitions. Phys. Rev. B **17**, 1302–1322 (1978)
31. Grest, G.S., Kremer, K.: Molecular dynamics simulations for polymers in the presence of a heat bath. Phys. Rev A **33**, 3628–3631 (1986)
32. Plimpton, S.: Fast parallel algorithms for short-range molecular dynamics. J. Comput. Phys. **117**, 1–19 (1995)
33. Fetters, L., Lohse, D., Richter, D., Witten, T., Zirkel, A.: Connection between polymer molecular weight, density, chain dimensions, and melt viscoelastic properties. Macromolecules **27**, 4639–4647 (1994)
34. Fetters, L.J., Lohse, D.J., Milner, S.T., Graessley, W.W.: Packing length influence in linear polymer melts on the entanglement, critical, and reptation molecular weights. Macromolecules **32**, 6847–6851 (1999)

35. Vega, J.F., Rastogi, S., Peters, G.W.M., Meijer, H.E.H.: Rheology and reptation of linear polymers. Ultrahigh molecular weight chain dynamics in the melt. J. Rheol. **48**, 663–678 (2004)
36. Hsu, H.-P., Kremer, K.: Static and dynamic properties of large polymer melts in equilibrium. J. Chem. Phys. **144**, 154907 (2016)
37. Peters, B.L., Salerno, K.M., Ge, T., Perahia, D., Grest, G.S.: Viscoelastic response of dispersed entangled polymer melts. Macromolecules **53**, 8400–8405 (2020)
38. Treloar, L.R.G.: The Physics of Rubber Elasticity. Oxford University Press, Oxford (1975)
39. Kremer, K., Grest, G.S.: Dynamics of entangled linear polymer melts: a molecular-dynamics simulation. J. Chem. Phys. **92**, 5057–5086 (1990)
40. Likhtman, A.E., McLeish, T.C.: Quantitative theory for linear dynamics of linear entangled polymers. Macromolecules **35**, 6332–6343 (2002)
41. Marrucci, G.: Relaxation by reptation and tube enlargement: a model for polydisperse polymers. J Polym. Sci. B **23**, 159–177 (1985)
42. Hou, J.-X., Svaneborg, C., Everaers, R., Grest, G.S.: Stress relaxation in entangled polymer melts. Phys. Rev. Lett. **105**, 068301 (2010)

Authors and Affiliations

Sidath Wijesinghe[1] · Dvora Perahia[1] · Ting Ge[2] · K. Michael Salerno[3] · Gary S. Grest[4]

[1] Department of Chemistry, Clemson University, Clemson, SC 29634, USA

[2] Department of Chemistry and Biochemistry, University of South Carolina, Columbia, SC 29208, USA

[3] U. S. Army Research Laboratory, Aberdeen Proving Grounds, Aberdeen, MD 21005, USA

[4] Sandia National Laboratories, Albuquerque, NM 87185, USA